JMEPEG (2007) 16:109–112
DOI: 10.1007/s11665-006-9017-8

1059-9495/$19.00

Effects of Isothermal Ageing and Continuous Cooling after Solubilization in a Duplex Stainless Steel

I. Calliari, M. Zanesco, E. Ramous, and P. Bassani

(Submitted February 10, 2006; in revised form April 12, 2006)

The kinetics of precipitation of secondary phases in a duplex stainless steel (SAF 2205) after isothermal and continuous cooling treatment were investigated. The evolution of the phases chemical composition in relation with time and cooling rate is presented.

Keywords continuous cooling, heat treating, intermetallics, stainless steels

1. Introduction

Duplex stainless steels (DSS) have an austenitic-ferritic microstructure that gives them a very good combination of mechanical and corrosion properties, at a competitive cost. A typical property of DSS is the high pitting resistance that makes them suitable for structural applications in very aggressive environments. However the use of DSS is limited by their susceptibility to the formation of dangerous intermetallic phases, such as σ-phase and χ-phase, resulting in detrimental effects on impact toughness and corrosion resistance. Therefore, many standards, relating to manufacturing of DSS, require "no intermetallic phases" in the microstructure.

To this end, DSS are submitted to a solution treatment, followed by water quenching, if and where it is possible. The aim of this treatment is not only to redissolve the dangerous phases and to avoid their precipitation in the 600–900 °C temperature range, but also to restore the ferrite/austenite ratio to approximately equal amounts, corresponding to the best mechanical and corrosion properties for the DSS.

The precipitation of secondary phases in these steels have received considerable attention. In spite of that, the mechanism of secondary phases formation is not definitely understood, and several precipitation sequences have been suggested (Ref 1-9). Most of the researches examine the precipitation during isothermal ageing treatments. The obtained results, therefore, are useful to define both the minimum temperature to dissolve the secondary phases and the maximum possible temperature suitable for applications of DSS, to avoid the precipitation of these phases during service. Little information, however, is available concerning the secondary phases formation during continuous cooling of DSS (Ref 10–12). The interesting topic is to define the minimum cooling rate sufficient to avoid the phases precipitation during cooling, after the solution treatment or welding.

In this paper, the formation of secondary phases in the most common DSS steel, the 2205 grade, has been examined, during both continuous cooling and isothermal treatments, to compare and define times and sequences of precipitation in the two different conditions. The secondary phases were detected and analyzed using the Scanning Electron Microscope (SEM) and the Energy-Dispersive X-ray Spectroscopy (EDS), as described in a previous work (Ref 13).

2. Experimental

As received material was a wrought SAF 2205 DSS rod (30 mm), with chemical composition reported in Table 1. Isothermal ageing treatments of specimens, previously solubilized at 1050 °C for 30 min, were carried out in the temperature range 780–900 °C. Relatively short ageing times were chosen to measure low amounts of secondary phases and investigate their precipitation kinetics.

Continuous cooling tests have been performed in a Setaram "Labsys TG" machine, in Argon atmosphere. Samples (diameter 6 mm, length 8 mm) were heated at 10 °C/min from room temperature and solution treated (maintenance for 5 min) at temperatures of 1020°C and 1050 °C, then cooled in argon at various cooling rates in the range 0.02–0.4 °C/s

Different phases have been identified by SEM-BSE examination of unetched samples. The ferrite appears slightly darker than austenite, while the secondary phases are lighter. Owing to the higher content of molybdenum, in combination with the large atomic scattering factor of molybdenum χ-phase appears in brighter contrast than σ-phase (Ref 1). The amount of secondary phases have been determined using image analysis software on SEM-BSE micrographs (10 fields, 1000×). The contribution of each phase to the total volume fractions was determined. The chemical composition of the phases was determined by SEM-EDS on unetched samples. The volume fractions of ferrite and austenite in a solution treated sample have been measured on 3 longitudinal and 3 transversal sections (20 fields for each section) by image analysis on light micrographs at 200×, after etching with the Beraha's reagent (R.T., 10s).

I. Calliari, M. Zanesco, and **E. Ramous,** Department of Innovation in Mechanics and Management (DIMEG), University of Padova, via Marzolo 9, 35131 Padova, Italy. **P. Bassani,** National Research Council – Institute for Energetics and Interphases, CNR-IENI Unit of Lecco, Corso Promessi Sposi 29, Lecco 23900, Italy. Contact e-mail: irene.calliari@unipd.it.

Table 1 Chemical composition (wt.%) of the SAF 2205

C	Si	Mn	Cr	Ni	Mo	P	S	N	Fe
0.03	0.56	1.46	22.75	5.04	3.19	0.025	0.02	0.16	Bal

3. Results and Discussion

3.1 Solution Treatment

At all the solubilization temperatures, the microstructure obtained for the treated material (in particular the ferrite/austenite ratio) was typical of the DSS rolled products. The banded structure of elongated γ-phase islands was observed in the longitudinal section, while the isotropic structure of ferrite and austenite grains was displayed on the transverse section. The values of volume fractions of ferrite and austenite, measured on longitudinal and transverse sections (200×), are typical of the steel considered: 53% of ferrite and 47% of austenite. The differences between transversal and longitudinal data are less than standard deviations. Therefore all the quantifications were performed on the transverse sections. Secondary phases were not detected in the solubilized material before the isothermal aging.

3.2 Isothermal Ageing

In the SEM-BSE images of the samples, after isothermal aging, ferrite and austenite appear in the background, with the ferrite darker than the austenite. The secondary phases appear as small bright regions (the χ-phase is brighter than the σ-phase). The observed precipitation sequence can be summarized as follows:

- 780 °C ageing: the first precipitates appear after 30′ ageing and become more evident after 40′, as in Fig. 1(a). The small bright particles were identified as χ-phase by the SEM-EDS, just within the beam resolution limit.
- 850 °C ageing: the v-phase appears after about 10′, while the r-phase after about 20′; After 30′ the v-phase and the r-phase are both present: the v-phase is always at the boundaries γ/α and α/α. The r-phase penetrates the ferrite or grows along the γ/α boundary as evidenced in Fig. 1(b).
- 900 °C ageing: also at this temperature the first precipitating phase is the v-phase, generally decorating the grain boundaries. By increasing the holding time, the amount of v-phase increases and also the r-phase appears, in the form of coarser precipitates at the γ/α boundary, but growing into the ferrite (Fig. 1c). Although σ particles are, at the beginning, less numerous than the χ-phase particles, they are coarser, and grow more rapidly, quickly reaching almost the same volume fraction. By increasing the holding time, σ-phase grows to large particles, moving from the boundaries into the ferrite, embedding some small χ particles. This seems to show the progressive transformation of χ-phase to σ-phase.During isothermal ageing, the χ-phase always appears as the first phase in the temperature range considered and is later followed by the σ-phase. The localization of the new phases at the ferrite/austenite boundaries is well known (Ref 1). Generally the secondary phases formation at the grain boundaries and the growth into ferrite are justified by the diffusion behavior of the elements involved in the transformation: the Mo diffusion coefficient is higher than the Cr and Ni ones and is also higher in ferrite than in austenite (Ref 4). Moreover, recent studies state that, at 900 °C the v-phase, formed at the lowest soaking times, is a meta-stable phase (Ref 3, 9) and is completely transformed into σ-phase after a long isothermal ageing. The formation of the v as the first meta-stable phase is justified by its cubic lattice and lower coherency strains with the parent cubic phases (Ref 1). Our results confirm that the transformation of χ-phase to σ-phase is faster at 900 °C, as the diffusion coefficients of Mo and Cr are higher than at 850 °C, and the lattice arrangement from cubic v-phase to tetragonal r-phase is favored. Moreover,

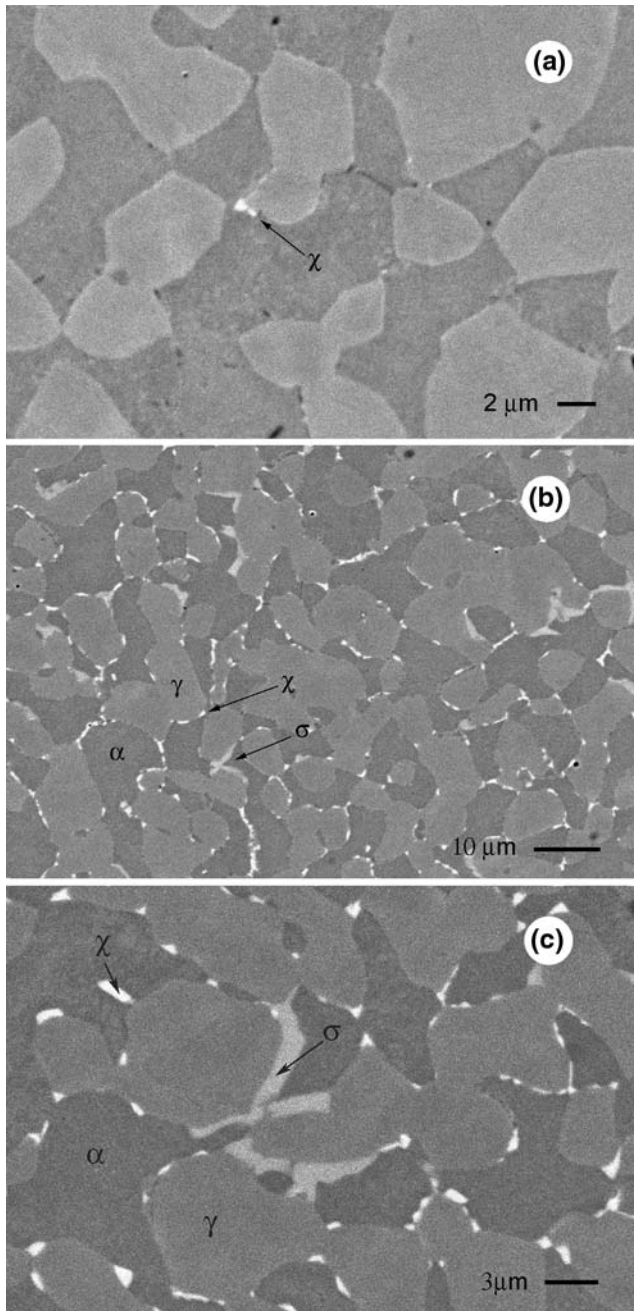

Fig. 1 SEM-BSE micrographs taken after 40′ at 780 °C (a), 30′ at 850 °C (b), 30′ at 900 °C (c)

these considerations confirm and suggest that v particles could act as preferential sites for the r-phase nucleation (Ref 1).

3.3 Continuous Cooling after Solubilization

The morphology and localization of the new phases after continuous cooling are very similar to that observed in the isothermal ageing tests (the precipitation occurs at the α/γ grain boundaries and especially at the triple points), while the formation sequence of secondary phases seems to be different.

The total amount of secondary phases is lower for the highest solubilization temperature, in agreement with (Ref 10), and is strongly dependent both on the cooling rates and on the solubilization temperature (see Fig. 2a, b). At the highest cooling rates the secondary phases precipitation is completely avoided. As the cooling rate slows down, the σ-phase appears as the first phase: the critical cooling rate for σ-phase formation is 0.35 °C/s, when a final σ-phase content of 0.2% is obtained. With a further lowering of the cooling rate, the σ-phase content gradually increases and at about 0.1–0.15 °C/s a small amount of χ-phase appears: therefore the χ-phase appears only at lower cooling rates than the σ-phase.

The final amount of both σ-phase and χ-phase is strongly dependent on the solubilization temperature, but in different ways. The σ-phase amount is higher in the samples treated at 1020 °C, the lowest solubilization temperature considered. On the contrary, the χ-phase amount is larger in the samples quenched from 1050 °C, the highest temperature considered.

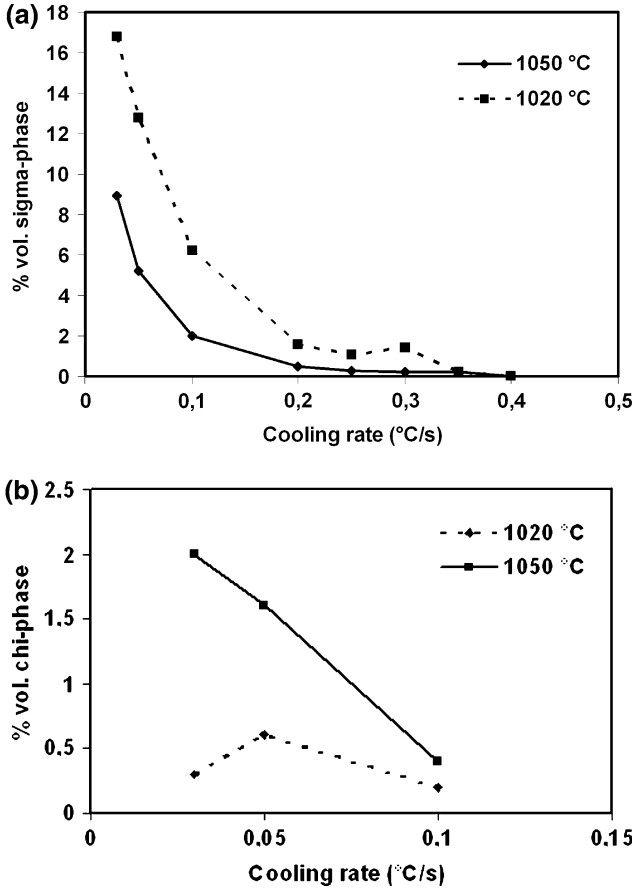

Fig. 2 (a) σ-phase volume fractions precipitated after different (1020 and 1050 °C) solubilization temperatures. (b) χ-phase volume fractions precipitated after different (1020 and 1050 °C) solubilization temperatures

These results indicate that the sequence of precipitation during continuous cooling can be different from that obtained by isothermal ageing. In the latter, the χ-phase is always the first precipitating phase, as metastable "precursor" of the stable σ-phase. In the continuous cooling, the same sequence occurs only at low cooling rates, and at the highest cooling rate the χ-phase formation seems to be not possible.

3.4 Secondary Phases Composition

Further information on the secondary phases precipitation in SAF 2205 steel can be derived from the chemical composition of the phases, after the different heat treatments considered.

The compositions of χ-phase and σ-phase after isothermal ageing (Table 2) and continuous cooling treatments (Tables 3 and 4) are in good agreement with the results of other investigations (Ref 6, 10). The χ-phase composition is characterized by a significant high content of molybdenum, nearly twice the Mo content of the σ-phase. Therefore, it is quite easy to distinguish these two phases through SEM-BSE imaging.

It is interesting to point out that after isothermal ageing the chemical composition of both χ-phase and σ-phase is independent of the time, the temperature, and the phase amount. Moreover the σ-phase composition is near the equilibrium phase composition (Ref 1).

On the contrary, the compositions of the secondary phases from continuous cooling tests are significantly dependent on the solubilization temperature and mainly on the cooling rates (Tables 3, 4). As the cooling rate decreases, in both σ- and χ-phases the molybdenum and chromium contents gradually increase, approaching the values obtained in the isothermal tests.

The most significant variation concerns the molybdenum content. The σ-phase Mo content varies from 4.6%, at the highest cooling rate, to 8%, at the lowest cooling rate. Given that the base alloy contains about 3% Mo, the large composition variation can be justified considering that the σ-phase and χ-phase formation is strongly dependent on diffusion. At the highest cooling rates there is not sufficient time for diffusion to supply adequate molybdenum (and chromium) amounts to reach the equilibrium composition. Therefore, the highest cooling rates produce σ-phase at the lowest alloying elements content.

Table 2 Chemical composition (wt.%) of χ-phase and σ-phase after isothermal ageing

Element	σ-phase	χ-phase
Mo	7.5 ± 0.8	13.0 ± 0.9
Cr	26.7 ± 1.1	24.0 ± 0.7
Ni	1.4 ± 0.1	3.6 ± 0.1

Table 3 Mo, Cr and Ni content (wt.%) of χ-phase after solubilization at 1020 °C and 1050 °C and continuous cooling treatment

	Solubilization at 1020 °C/s			Solubilization at 1050 °C/s		
Cooling rate °C/s	Mo	Cr	Ni	Mo	Cr	Ni
0.03	14.3	25.2	2.7	15.2	26.0	2.9
0.05	11.8	25.2	2.9	16.1	25.7	3.0
0.10	11.2	24.3	3.3	12.0	26.1	3.5

Table 4 Mo, Cr and Ni content (wt.%) of σ-phase after solubilization at 1020 °C and 1050 °C and continuous cooling treatment

Cooling rate °C/s	Solubilization at 1020 °C			Solubilization at 1050 °C		
	Mo	Cr	Ni	Mo	Cr	Ni
0.03	8.4	28.5	3.1	7.8	28.7	2.9
0.05	7.3	27.2	3.3	8.0	28.8	3.0
0.10	7.3	27.3	3.0	7.5	25.9	3.5
0.20	7.3	27.3	3.0	7.3	27.5	3.2
0.25	6.1	25.5	3.7	8.3	26.6	3.3
0.30	6.1	25.1	4.0	6.8	27.0	3.5
0.35	5.6	25.4	3.9	7.0	26.1	3.8

This effect (σ-phase with low molybdenum content at the highest cooling rates) is more evident in samples quenched from 1020 °C than in those quenched from 1050 °C. In this case, the samples spent more time at high temperatures, and this favors the alloying elements diffusion towards the precipitation sites.

The more evident variation of the χ-phase composition follows the same behavior and can be justified in the same way. Owing to its high molybdenum content, the formation of the χ-phase is even more affected by the restriction of the time for diffusion. The χ-phase appears only in the precipitation conditions with the longest time allowed for diffusion: isothermal ageing and the lowest cooling rates. This behavior could be justified because the χ-phase nucleation is favored by smaller coherency strains than σ-phase in the ferrite lattice. In fact, the χ-phase has a cubic lattice and a well-defined orientation relationship with the host lattice ($\langle 001\rangle_\chi // \langle 001\rangle_\alpha$) (Ref 3). On the contrary, the χ-phase formation is not favored by the high molybdenum content, requiring a more effective diffusion. Therefore, in experimental conditions with the longest diffusion time, i.e. isothermal tests and low cooling rates, the nucleation prevails and the χ-phase appears as the first precipitating phase.

On the contrary, at the highest cooling rates the insufficient time for diffusion prevails and prevents the χ-phase formation: it is observed, therefore, only the formation of the final and stable σ-phase. The effect of diffusion on the possible χ-phase formation is further confirmed by the significantly high χ-phase amounts obtained in the samples quenched from the highest solubilization temperature (1050 °C), but always at the lowest cooling rates.

These results seem to indicate that the role of the χ-phase, as the stable σ-phase precursor in the DSS, is not a general phenomena, but depends on the steel composition (mainly on the molybdenum content) and can occur only with specific conditions of solubilization temperature or cooling rates. This, perhaps, could also justify some discrepancies between various results already reported (Ref 6, 8-10), concerning the sequence of secondary phases formation in DDS.

4. Conclusions

In the SAF 2205 DSS the precipitation of secondary phases (in particular σ and χ-phase) after isothermal and continuous cooling treatment was investigated.

- the precipitation sequence is different in the two situations: during isothermal ageing the χ-phase always precipitates before the σ-phase, but, during continuous cooling, the χ-phase appears only at low cooling rates;
- the chemical composition of both secondary phases varies with the cooling rate: increasing the cooling rate the molybdenum and chromium content in the precipitating phase decreases;
- the chemical composition variation of both precipitating phases puts in evidence the influence of the diffusion which controls the precipitation: the formation of the χ-phase, as metastable "precursor" of the stable σ-phase, is possible and occurs only in treatments with the longest time for diffusion: isothermal ageing and low cooling rates.

References

1. J.O. Nilsson, Super Duplex Stainless Steels, *Mat. Sci. Techn.*, 1992, **8,** p 685–700
2. J.O. Nilsson, T. Huhtala, P. Jonsson, L. Karlsson, and A. Wilson, Structural Stability of Duplex Stainless Weld Metals and its Dependence on Tungsten and Copper, *Metall*, 1996, **27A,** p 2196–2208
3. J.O. Nilsson, The Physical Metallurgy of Duplex Stainless Steels, Proceedings of Conference "Duplex Stainless Steel 97", Stainless Steel World, KCI publishing, 1997, p 73–81
4. R.N. Gunn, (2000) Reduction in Fracture Toughness due to Intermetallic Precipitates in Duplex Stainless Steels, *Proceedings of the Conference "Duplex America 2000"*, Stainless Steel World, KCI Publishing, p 299–314
5. L. Karlsson, L. Bengtsson, U. Rolander, S. Pak, Kinetics of Intermetallic Phase Formation in Duplex Stainless Weld Metals and their Influence on Mechanical Properties, *Proceedings of Conference "Application stainless steel 92"*, Stockholm, The Institute of Metals, 1992, p 335–344
6. T.H. Chen, K.L. Weng, and J.R. Yang, The Effect of High-Temperature Exposure on The Microstructural Stability and Toughness Property in A 2205 Duplex Stainless Steel, *Mat. Sci. Eng.*, 2002, **A338,** p 259–270
7. L. Duprez, B.C. Cooman, N. Akdut, Microstructural Changes in Duplex Stainless Steel during Isothermal Annealing, *Proceedings of the Conference "Duplex 2000"*, Venice, edited by Italian Association of Metallurgy (AIM), 2000, p 355–365
8. K.M. Lee, H.S. Cho, and D.C. Choi, Effect of Isothermal Treatment of SAF 2205 Duplex Stainless Steel on Migration of δ/γ Interface Boundary and Growth of Austenite, *J. Alloys Comp.*, 1999, **285,** p 156–161
9. Y.S. Ahn and J.P. Kang, Effect of Aging Treatments on Microstructure and Impact Properties of Tungsten Substituted 2205 Duplex Stainless Steel, *Mat. Sci. Techn.*, 2000, **16,** p 382–388
10. T.H. Chen and J.R. Yang, Effects of Solution Treatment and Continuous Cooling on σ-Phase Precipitation in a 2205 Duplex Stainless Steel, *Mat. Sci. Eng.*, 2001, **A311,** p 28–41
11. S.B. Kim, K.W. Paik, and Y.G. Kim, Effect of Mo Substitution by W on High Temperature Embrittlement Characteristics in Duplex Stainless Steels, *Mat. Sci. Eng.*, 1998, **A247,** p 67–74
12. E. Johnson, Y.J. Kim, L. Scott Chumbley, and B. Gleeson, Initial Phase Transformation Diagram Determination for the CD3MN Cast Duplex Stainless Steel, *Scri. Mat.*, 2004, **50,** p 1351–1354
13. I. Calliari, M. Magrini, and E. Ramous, Measurements of Secondary Phases Content in a 22Cr5Ni Duplex Stainless Steel, *Praktische Metallographie/Practical Metallography*, 2005, **42,** p 74–88